

# QCD THERMODYNAMICS AND THE POLYAKOV LOOP\*

KENJI FUKUSHIMA

Yukawa Institute for Theoretical Physics, Kyoto University  
Kitashirakawa Oiwake-Cho, Kyoto 606-8502, Japan

(Received January 27, 2010)

We discuss the phase diagram of QCD at finite temperature  $T$  and baryon chemical potential  $\mu_B$  using the Polyakov-loop coupled Nambu–Jona-Lasinio (PNJL) model. We propose a way to prescribe the phase diagram by means of the thermodynamic quantities. We find that the resulting phase diagram is consistent with the conventional one defined by the chiral condensate and the Polyakov loop.

PACS numbers: 12.38.Aw, 11.10.Wx, 11.30.Rd

## 1. Introduction

Phase transitions of QCD matter at finite temperature  $T$  and baryon density or chemical potential  $\mu_B$  have been of much interest in theory and experiment on the relativistic heavy-ion collisions. It has been established that, when  $\mu_B$  is much smaller than  $T$ , strongly interacting matter undergoes a phase transition at  $T$  that is comparable to the QCD energy scale  $\Lambda_{\text{QCD}} \sim 200$  MeV. The phase transition is usually characterized by two approximate order parameters, *i.e.* the (traced) Polyakov loop  $\ell = 1/3\langle\text{Tr}L\rangle$  and the chiral condensate  $\langle\bar{q}q\rangle$ . Although they happen to indicate a common transition temperature,  $\ell$  and  $\langle\bar{q}q\rangle$  belong to completely different dynamics in QCD; the Polyakov loop is a good order parameter for *quark deconfinement* in the quenched ( $m_q \rightarrow \infty$ ) limit, while the chiral condensate for *chiral restoration* in the chiral ( $m_q \rightarrow 0$ ) limit.

One may wonder that a rapid crossover in one side (quark deconfinement for example) could be a trigger for transitional behavior in the other side (chiral restoration for the same example). This is partially the case indeed. The Polyakov loop and the chiral condensate have a quantum number  $0^{++}$

---

\* Talk presented at the EMMI Workshop and XXVI Max Born Symposium “Three Days of Strong Interactions”, Wrocław, Poland, July 9–11, 2009.

the same as that of the vacuum, so that they both describe the  $0^{++}$  glueball and the scalar–isoscalar (so-called  $\sigma$ ) meson states, which can be mixed up with each other. Because of mixing, it is natural to anticipate simultaneous increase or decrease in the order parameters as a function of  $T$  and  $\mu_B$  [1, 2]. This explanation is not really adequate to give a full account for what has been observed in the lattice QCD simulations [3].

In the density region where the Monte Carlo simulation is feasible it has been found that  $\ell$  and  $\langle \bar{q}q \rangle$  are monotonically increasing and decreasing, respectively, as  $T$  goes from below to above  $T_c$  which is common to both order parameters. This observation is something more than implied by mixing. In general, the mixing argument cannot exclude a possibility that there appear two separate crossovers with one dominated by deconfinement and another by chiral restoration. The fact is, however, that quark deconfinement and chiral restoration should take place at the same or nearly the same temperature. Two phenomena that are originally opposite to each other with respect to  $m_q$  must be locked together for a wide range of intermediate quark mass,  $0 < m_q < \infty$  [4].

Attempts to resolve this question about underlying mechanism in order to link quark deconfinement and chiral restoration include a double expansion of strong coupling constant and large dimensions. This was performed to build an effective model in terms of both order parameters [5–8]. The strong-coupling model was so successful that it could reproduce qualitative behavior of  $\ell$  and  $\langle \bar{q}q \rangle$  in a similar way to the finite- $T$  lattice QCD simulation. It was not easy, however, for the model to go beyond qualitative agreement and to say anything quantitative. This is so because the model was formulated on the lattice which is far from the continuum limit. Besides, hopping of quarks in the spatial directions is suppressed by the strong coupling constant and all quark excitations are static in configuration space (straight along the temporal direction). The Fermi surface, hence, cannot be formed correctly even with a finite  $\mu_B$  introduced. Moreover, it is non-trivial how to recover the Stefan–Boltzmann law at extremely high  $T$  due to the presence of dimensional scale other than  $T$ , that is, a lattice spacing or an ultraviolet (UV) cutoff.

The chiral sector of the strong-coupling model in the leading order of the double expansion turns out to be an effective description in terms of quarks with four-fermion vertices. This is reminiscent of a chiral effective model with a UV cutoff, known as the Nambu–Jona-Lasinio (NJL) model [9, 10]. After revisiting the strong-coupling model [7, 8] it had not been so long before an idea was proposed that the NJL model is naturally augmented with the Polyakov loop  $\ell$  in a way inspired by the strong-coupling expansion [11]. Such a hybrid model with the Polyakov loop coupling is called the PNJL model [12].

Although the PNJL model originally aimed to explain the simultaneous crossovers of quark deconfinement and chiral restoration, a bonus has been recognized that thermodynamic quantities such as the pressure, the entropy density, the quark number susceptibility, *etc.* are in good agreement with the results from the lattice simulation *with dynamical quarks* once the model parameters are fixed by the lattice data *without quarks* [12]. Since the lattice QCD simulation is unable to access high- $\mu_B$  and low- $T$  regions hindered by the sign problem, the PNJL model is quite useful there. As we will see later, one important prediction from the PNJL model is that two phase boundaries of deconfinement and chiral crossovers may get apart from each other as  $\mu_B$  increases [11, 14].

When it comes to the phase structure, the existence or location of the chiral critical point of QCD is also of great interest [15, 16]. We mention on the fact that the existence or location of the QCD critical point can be drastically affected by slight changes in PNJL model studies [17]. In this article we rather focus on another special point on the phase structure, namely, a region that looks like a triple point. We will propose a prescription to draw the phase diagram using the entropy density and the baryon number density. In this way we shall understand a physical meaning of the triple-point-like region intuitively.

## 2. Polyakov loop and physical degrees of freedom

It is quite non-trivial whether the PNJL model can reproduce full QCD thermodynamics around  $T_c$ . This is because the Polyakov loop is expressed in terms of longitudinal  $A_4$  (temporal component of the gauge field) only, while the thermally excited gluons are transverse  $A_i$  in the perturbative regime. In fact, the Polyakov loop is so influential to colored objects that it can control the thermal excitation of transverse gluons as well as quarks. In what follows let us discuss the Polyakov loop coupling with quarks and transverse gluons in order.

### 2.1. Quarks

If we assume the mean-fields to incorporate interaction effects (*i.e.* quasi-particle approximation), the grand-canonical partition function for quasi-quarks is

$$Z_{\text{quark}} = \prod_{i,p} \left[ 1 + e^{-(E_i(p) - \mu_q)/T} \right] \left[ 1 + e^{-(E_i(p) + \mu_q)/T} \right], \quad (1)$$

where  $i$  runs over 3 colors, 3 (or 2) flavors, and 2 spin states. A quark chemical potential  $\mu_q = \mu_B/3$  instead of  $\mu_B$  is used above. We did not consider the Polyakov loop coupling yet. The Polyakov loop,  $L$ , is a  $3 \times 3$

matrix in color space associated with thermal quark propagation, which represents a color-screening phase factor. Therefore, the covariant coupling with the  $A_4$  field leads to a coupling of  $L$  and  $L^\dagger$  with the thermal Boltzmann factor as

$$\begin{aligned} Z_{\text{quark}} &= \prod_{i,p} \det \left[ 1 + L e^{-(E_i(p)-\mu_q)/T} \right] \left[ 1 + L^\dagger e^{-(E_i(p)+\mu_q)/T} \right] \\ &= \prod_{i,p} \left[ 1 + 3\ell e^{-(E_i-\mu_q)/T} + 3\bar{\ell} e^{-2(E_i-\mu_q)/T} + e^{-3(E_i-\mu_q)/T} \right] \\ &\quad \times \left[ 1 + 3\bar{\ell} e^{-(E_i+\mu_q)/T} + 3\ell e^{-2(E_i+\mu_q)/T} + e^{-3(E_i+\mu_q)/T} \right]. \quad (2) \end{aligned}$$

Here we note that  $\ell$  denotes the traced Polyakov loop  $\ell = 1/3 \text{Tr} L$  and  $\bar{\ell}$  the anti-Polyakov loop  $\bar{\ell} = 1/3 \text{Tr} L^\dagger$ . At zero baryon density  $\bar{\ell}$  is just identical with  $\ell$ , but once a finite density is turned on,  $\bar{\ell} > \ell$  for positive  $\mu_q$  because an antiquark is more efficiently screened in a medium with quarks. Each term has a clear physical meaning in Eq. (2); in the angle brackets the first term without the Boltzmann factor represents no particle excitation, the second term proportional to  $e^{-(E_i-\mu_q)/T}$  a single particle excitation, the third term proportional to  $e^{-2(E_i-\mu_q)/T}$  a two-particle or a diquark-like excitation in the color antitriplet channel, and the last term a colorless baryon-like excitation.

Just to demonstrate how the Polyakov loop coupling controls thermal excitations we shall compute the quark pressure  $p_{\text{quark}} = TV^{-1} \ln Z_{\text{quark}}$  from the partition function (2) in which the quark mass and chemical potential are set to be zero so that the pressure is simply proportional to  $T^4$ . Then, in the free-quark limit (*i.e.*  $\ell = \bar{\ell} = 1$ ), the Stefan–Boltzmann law reads  $p_{\text{free}} = (63\pi^2/180)T^4$  for massless three flavors. We measure the quark pressure in the unit of the Stefan–Boltzmann value;  $\nu = p_{\text{quark}}/p_{\text{free}}$ , which actually counts the relevant degrees of freedom. We plot  $\nu$  as a function of  $\ell$  in the simple case with  $m_q = \mu_q = 0$  in the left of Fig. 1. It is apparent that the pressure contribution is non-zero but nearly vanishing at  $\ell = 0$  and is almost linearly increasing as  $\ell$  becomes larger. If we recall that the Polyakov loop is an order parameter for quark deconfinement, we can naturally understand this; no pressure from quarks in the confined phase at  $\ell = 0$  and the free-quark limit is reached in the deconfined phase at  $\ell = 1$ . It should be mentioned here that the colorless baryon-like term in Eq. (2) remains even at  $\ell = 0$  but its contribution to the pressure is suppressed by a factor  $1/3^4 = 0.012$  as compared to the free-quark excitation.

## 2.2. Transverse gluons

From the theoretical argument based on center symmetry in the pure gluonic sector, the traced Polyakov loop in the color fundamental representation serves as an order parameter for *quark* deconfinement (but not for

gluon deconfinement). Because gluons can screen other gluons, a long-range confining force between gluons is saturated by string breaking due to two glueball excitations even when color charge is strictly confined. Thus, it is not clear *a priori* whether  $\ell$  can be useful to parametrize the pressure from transverse gluons.

In the same manner as in the quark case we can consider the grand-canonical partition function for quasi-gluons, that is,

$$Z_{\text{gluon}} = \prod_{i,p} \det \left[ 1 - L_{\text{adj}} e^{-p/T} \right], \tag{3}$$

where  $i$  runs over 8 colors and 2 transverse polarizations. Here we introduced  $L_{\text{adj}}$  to denote an  $8 \times 8$  Polyakov loop matrix in the color adjoint representation. In the Stefan–Boltzmann limit with  $L_{\text{adj}} = 1$ , the pressure is  $p_{\text{free}} = (16\pi^2/90)T^4$ . Again, the gluon pressure is calculated from Eq. (3) in the unit of the Stefan–Boltzmann value and the numerical result is shown in the right part of Fig. 1. The pressure dependence on  $\ell$  is not linear this time but almost quadratic reflecting the fact that the adjoint Polyakov loop is expressed as  $\{L_{\text{adj}}\}_{ab} = 2\text{Tr}[t_a L t_b L^\dagger]$  in terms of the fundamental one.

It might be appropriate here to explain some more details on the evaluation of the transverse pressure. Unlike the quark contribution (2) we cannot rewrite the gluon pressure (3) only in terms of  $\ell$  and  $\bar{\ell}$ . It requires us, therefore, to adopt an elaborated procedure for the mean-field approximation [5, 7, 18–21]. Then, a mean-field weight factor is introduced as  $e^{-S_{\text{mf}}} = \prod e^{x \text{Tr} L}$ , so that the expectation value of the fundamental Polyakov loop,  $\ell(x) = \int dL 1/3 \text{Tr} L e^{x \text{Tr} L} / \int dL e^{x \text{Tr} L}$  takes a nonzero value proportional to a mean-field variable  $x$  (that is;  $x$  is a source conjugate to  $\ell$ ). In the same way the gluon pressure is numerically calculated as a function of  $x$ , from which we can eliminate the  $x$ -dependence using  $\ell = \ell(x)$ .

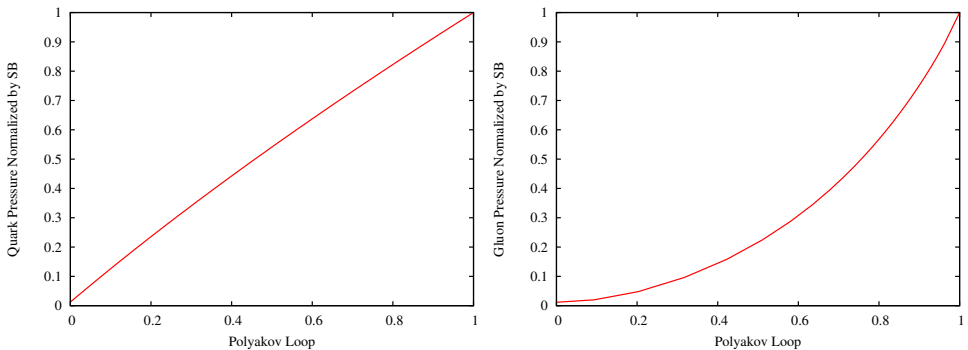


Fig. 1. Pressure contributions from quasi-quarks (left) and quasi-gluons (right) as a function of the traced Polyakov loop  $\ell$  in the color fundamental representation.

It is surprising that a Polyakov loop value as large as 0.8 yields a transverse pressure less than 0.6 times the Stefan–Boltzmann value. The right part of Fig. 1 manifests the importance of the Polyakov loop even in the deconfined region where  $\ell$  is substantially large but do not yet reach unity. In this region the screening effect by the Polyakov loop overwhelmingly governs the degrees of freedom allowed in the system, which would cause non-perturbative deviations from the Stefan–Boltzmann limit regardless of the interaction strength. Such a highly non-trivial state of matter is sometimes referred to as a semi-quark–gluon plasma (semi-QGP) [22].

### 3. Thermodynamics in pure gluodynamics

So far we have seen that the Polyakov loop can control the thermal excitation even for transverse gluons which couple with the adjoint Polyakov loop which is always non-zero due to color screening by other gluons. It should be acceptable to parametrize the physical pressure only in terms of  $\ell$ , which can be justified by the observation in the right part of Fig. 1 that  $\ell$  is practically an order parameter for gluon deconfinement as well.

Therefore, we may well assume that the pressure in pure gluodynamics is a function of  $\ell$  with coefficients depending on  $T$ . A frequently used ansatz [23] is

$$V(\ell) = -\frac{1}{2} a(T) \ell \bar{\ell} + b(T) \ln [1 - 6 \ell \bar{\ell} + 4(\ell^3 + \bar{\ell}^3) - 3(\ell \bar{\ell})^2] , \quad (4)$$

where  $a(T)/T^4 = (3.51 - 2.47t^{-1} + 15.2t^{-2})$  and  $b(T)/T^4 = -1.75t^{-3}$  with  $t = T/T_c$ . There are three independent parameters in this ansatz because of a constraint that  $V(\ell = 1)$  should obey the Stefan–Boltzmann law. This form (4) is very similar to another ansatz with two parameters  $\alpha$  and  $\beta$  motivated by the strong coupling analysis;  $a(T)/T = 54\beta e^{-\alpha/T}$  and  $b(T)/T = \beta$ , where  $\beta$  has mass dimension 3 whose scale comes from the UV cutoff [11, 17]. In the vicinity of  $T_c$  both parametrizations end up with approximately same thermodynamics anyway.

From the stationary condition  $dV/d\ell = 0$  the Polyakov loop expectation value is extracted from Eq. (4), which is compared with the lattice data taken from Ref. [24] as presented in the left part of Fig. 2. Because of renormalization effect the Polyakov loop in the lattice simulation exceeds unity, while  $\ell$  never gets greater than unity. This is why the agreement looks worse at high temperature. We see, in contrast, that the fitting works nicely and the potential reproduces the thermodynamic quantities such as the pressure  $p$ , the entropy density  $s$ , and the internal energy density  $\varepsilon$  well. For the sake of comparison we plot the output from Eq. (4) and the lattice data taken from Ref. [25]. Now we have finished fixing the pure gluonic sector.

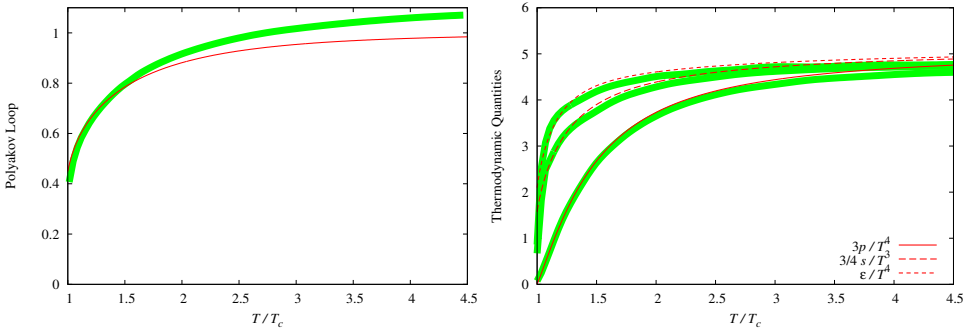


Fig. 2. Comparison between the quenched lattice data — thick curves (green) and the results from the potential ansatz — thin curves (red). The left part shows the Polyakov loop and the right part shows the thermodynamic quantities.

### 4. Thermodynamics with dynamical quarks

The quark sector is described by the NJL model which has three parameters, namely, the current quark mass  $m_u = m_d$ , the four-fermion coupling constant  $g_s$ , and the UV cutoff  $\Lambda$  for the two-flavor case, and two more parameters, namely, the strange quark mass  $m_s$  and the 't Hooft interaction strength  $g_d$  for the three-flavor case. The model parameters are fixed by the hadron properties;  $m_\pi$ ,  $f_\pi$ , and  $\langle \bar{q}q \rangle$  for two-flavor matter, and  $m_K$  and  $m_\eta'$  in addition for three-flavor matter.

The NJL model with the Polyakov loop coupling in Eq. (2) and the potential in Eq. (4) gives full thermodynamics in the plane spanned by  $T$  and  $\mu_B$ . We plot some of thermodynamic quantities in Fig. 3. The left part shows the entropy density that is  $s = -\partial\Omega/\partial T$  and the right part shows the baryon number density that is  $n_B = -\partial\Omega/\partial\mu_B$ . The reason why we chose

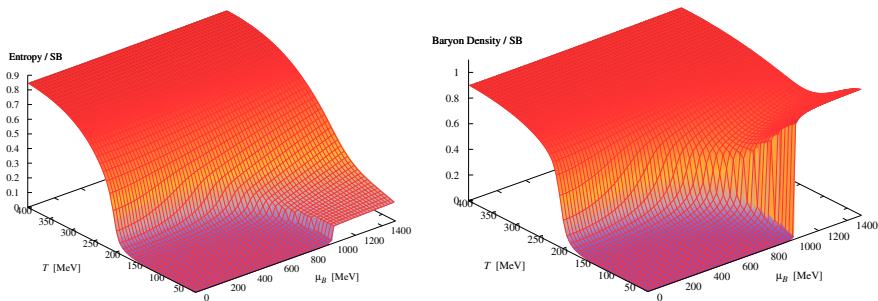


Fig. 3. Entropy density (left) and baryon number density (right) normalized by the Stefan–Boltzmann limit values as functions of  $T$  and  $\mu_B$  obtained in the three-flavor PNJL model.

them is that  $s$  and  $n_B$  should be suitable for detecting a change of the state of matter as  $T$  and  $\mu_B$  increases, respectively [26]. One can see that  $s$  is an increasing function of  $T$  whose dependence on  $\mu_B$  is mild, while  $n_B$  jumps drastically with increasing  $\mu_B$ . One possible interpretation is that  $s$  carries information on the deconfinement and  $n_B$  is an effective order parameter for the realization of so-called *quarkyonic* matter [27–29].

## 5. Phase diagram

The PNJL model is capable of dealing with  $\ell$  and  $\langle \bar{q}q \rangle$  both as  $T$  and  $\mu_B$  change, from which the phase diagram is deduced. The phase diagram in the context of the PNJL model was first depicted in Ref. [23], and in Ref. [14] it was clearly recognized that the deconfinement line characterized by the Polyakov loop (susceptibility) becomes distinct from the chiral transition line characterized by the chiral condensate (or susceptibility). The model has been extended to the three-flavor case later on [17,30,31]. In the presence of the Polyakov loop background it is not easy to take account of the diquark condensate. In Refs. [23,32,33] the diquark condensate has been considered in a gauge dependent treatment, but as pointed out in Ref. [32] such a treatment breaks color neutrality even in normal quark matter, which is unphysical artifact. A remedy is formulated in Ref. [21], but for technical reasons its application to the color-superconducting phase has not been done yet.

So far, in view of existing works on the phase diagram using the PNJL model [14, 17, 23, 30, 31] the robust prediction is that two separate phase boundaries appear on the phase diagram. A typical example is shown in Fig. 4.

This phase diagram is topologically the same as suggested by the large  $N_c$  argument [27–29]. In the region surrounded by two phase boundaries (which have finite width in Fig. 4 because they are both crossovers) the color degrees of freedom is confined because of  $\ell \simeq 0$  and chiral symmetry is restored and the Fermi sphere is filled by light quarks. Intuitive understanding on this peculiar state is as follows; the degenerated Fermi matter consists of light quarks and any excitation on top of the Fermi surface should be colorless like mesons and baryons.

In the left we show the phase diagram defined in a conventional way using the order parameters. The right of Fig. 4 is a phase diagram deduced from the entropy density and the baryon number density normalized by the Stefan–Boltzmann values. We see that the baryon density follows along the boundary of the chiral phase transition. This is because a transitional change in the constituent quark mass is attributed to a rapid jump in the baryon number density. Also we note that the entropy density is suppressed

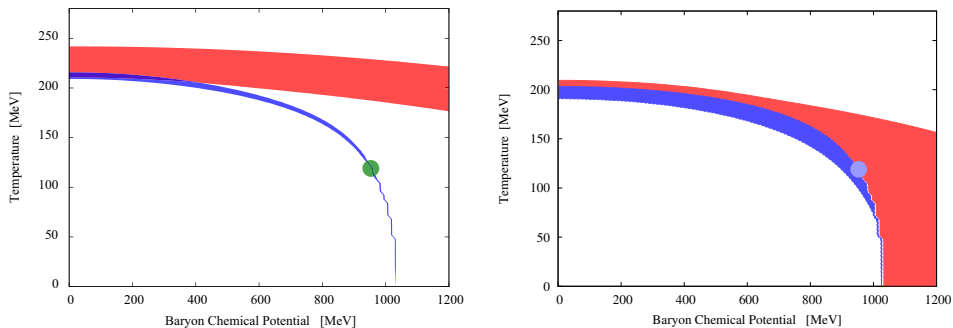


Fig. 4. Typical phase diagrams from the PNJL model. Left: The gray (red) band indicates a region in which  $\ell$  takes a value from 0.4 to 0.6 and the dark gray (blue) band a region in which  $\langle \bar{q}q \rangle / \langle \bar{q}q \rangle_0$  from 0.4 to 0.6. A circle locates the critical point below which the chiral phase transition is of the first order and the dark gray (blue) band has no width. Right: The gray (red) and dark gray (blue) bands represent a region where  $s$  and  $n_B$  in the unit of the Stefan–Boltzmann value take a value from 0.1 to 0.3, respectively.

as long as the Polyakov loop stays small, which is a natural consequence in the quark confined phase. Thus, we can conclude that it is reasonable to depict the phase diagram by means of the thermodynamic quantities.

Finally, we make a remark that this way of formulating the thermodynamic phase diagram has an advantage over the order parameters. That is, we can use a statistical model, for example, to extract the information on the phase boundary [26]. The statistical model is a hadronic description and thus it is not valid above  $T_c$ . Nevertheless, if the quark–hadron duality holds, there must be an overlapping region where both quark and hadron models are eligible. Since the statistical model is so successful to account for the observed particle ratios, it would be interesting to see the location of the phase boundaries implied by the model.

## REFERENCES

- [1] S. Digal, E. Laermann, H. Satz, *Eur. Phys. J.* **C18**, 583 (2001).
- [2] A. Mocsy, F. Sannino, K. Tuominen, *Phys. Rev. Lett.* **92**, 182302 (2004).
- [3] Y. Hatta, K. Fukushima, *Phys. Rev.* **D69**, 097502 (2004);  
arXiv:hep-ph/0311267.
- [4] F. Karsch, E. Laermann, A. Peikert, *Nucl. Phys.* **B605**, 579 (2001).
- [5] A. Gocksch, M. Ogilvie, *Phys. Rev.* **31**, 877 (1985).
- [6] E.M. Ilgenfritz, J. Kripfganz, *Z. Phys.* **C29**, 79 (1985).

- [7] K. Fukushima, *Phys. Lett.* **B553**, 38 (2003); *Phys. Rev.* **B68**, 045004 (2003).
- [8] K. Fukushima, *Prog. Theor. Phys. Suppl.* **153**, 204 (2004).
- [9] S.P. Klevansky, *Rev. Mod. Phys.* **64**, 649 (1992).
- [10] T. Hatsuda, T. Kunihiro, *Phys. Rep.* **247**, 221 (1994).
- [11] K. Fukushima, *Phys. Lett.* **B591**, 277 (2004).
- [12] C. Ratti, M.A. Thaler, W. Weise, *Phys. Rev.* **D73**, 014019 (2006).
- [13] C. Ratti, S. Roessner, W. Weise, *Phys. Lett.* **B649**, 57 (2007).
- [14] C. Sasaki, B. Friman, K. Redlich, *Phys. Rev.* **D75**, 074013 (2007).
- [15] M. Asakawa, K. Yazaki, *Nucl. Phys.* **A504**, 668 (1989).
- [16] A. Barducci, R. Casalbuoni, S. De Curtis, R. Gatto, G. Pettini, *Phys. Lett.* **B231**, 463 (1989); A. Barducci, R. Casalbuoni, G. Pettini, R. Gatto, *Phys. Rev.* **D49**, 426 (1994).
- [17] K. Fukushima, *Phys. Rev.* **D77**, 114028 (2008) [Erratum **D78**, 039902 (2008)].
- [18] E. Megias, E. Ruiz Arriola, L.L. Salcedo, *Phys. Rev.* **D74**, 065005 (2006).
- [19] K. Fukushima, Y. Hidaka, *Phys. Rev.* **D75**, 036002 (2007).
- [20] H.M. Tsai, B. Muller, *J. Phys. G* **36**, 075101 (2009).
- [21] H. Abuki, K. Fukushima, *Phys. Lett.* **B676**, 57 (2009).
- [22] Y. Hidaka, R.D. Pisarski, *Phys. Rev.* **D78**, 071501 (2008).
- [23] S. Roessner, C. Ratti, W. Weise, *Phys. Rev.* **D75**, 034007 (2007).
- [24] S. Gupta, K. Huebner, O. Kaczmarek, *Phys. Rev.* **D77**, 034503 (2008).
- [25] G. Boyd, J. Engels, F. Karsch, E. Laermann, C. Legeland, M. Lutgemeier, B. Petersson, *Nucl. Phys.* **B469**, 419 (1996).
- [26] K. Fukushima, Y. Hidaka, work under completion.
- [27] L. McLerran, R.D. Pisarski, *Nucl. Phys.* **A796**, 83 (2007).
- [28] Y. Hidaka, L.D. McLerran, R.D. Pisarski, *Nucl. Phys.* **A808**, 117 (2008).
- [29] L. McLerran, K. Redlich, C. Sasaki, *Nucl. Phys.* **A824**, 86 (2009).
- [30] W.J. Fu, Z. Zhang, Y.X. Liu, *Phys. Rev.* **D77**, 014006 (2008).
- [31] M. Ciminale, R. Gatto, N.D. Ippolito, G. Nardulli, M. Ruggieri, *Phys. Rev.* **D77**, 054023 (2008).
- [32] H. Abuki, M. Ciminale, R. Gatto, G. Nardulli, M. Ruggieri, *Phys. Rev.* **D77**, 074018 (2008).
- [33] D. Gomez Dumm, D.B. Blaschke, A.G. Grunfeld, N.N. Scoccola, *Phys. Rev.* **D78**, 114021 (2008).